



## Footfall dynamics for racewalkers and runners barefoot on compliant surfaces

James F. Wilson<sup>a,\*</sup>, Rodger D. Rochelle<sup>b</sup>

<sup>a</sup> Department of Civil and Environmental Engineering, Pratt School of Engineering, Duke University, 6319 Mimosa Drive, Chapel Hill NC 27514, United States

<sup>b</sup> North Carolina Department of Transportation, Project Services, 1591 Mail Service Center, Raleigh, NC 27699-1591, United States

### ARTICLE INFO

#### Article history:

Accepted 14 July 2009

#### Keywords:

Compliant surfaces  
Foot impact  
Leg damping  
Leg stiffness  
Racewalking  
Running

### ABSTRACT

The main purpose of this study is to investigate the role of footfall surface compliance on the physical parameters affecting barefoot racewalkers and runners. These parameters are identified using a new inverted pendulum body model with a forward moving foot pivot. Model correlations of footfall loads measured for four compliant surface mats showed leg–foot compression stiffness for both gaits were in the range of 10.8–12.9 kN/m, with the initial stiffness spikes in the range of 6.5–52 kN/m. The average leg damping factor was about 0.6% for racewalkers and 6% for runners. For both gaits there was negative leg damping just prior to foot lift-off. Compared to the peak reactions for the rigid surface, a mat of intermediate compliance (1020 kN/m) was effective in reducing the runners' peak reaction spikes by as much as 17%.

© 2009 Elsevier Ltd. All rights reserved.

### 1. Introduction

Racewalking is quite different from running. In racewalking the heel of the advancing foot contacts the ground before the rear foot leaves the ground, and the knee flexion in the supporting leg vanishes when this leg is vertical (Gray, 1985; Salvage, 2004). In running, however, the knee is bent during foot impact and that there is a momentary loss of contact of both feet with the ground during a flight phase (Seyfarth et al., 2003). Comparative studies of these gaits for subjects on rigid surfaces, with a historical review of related literature, were published by Cairns et al. (1986). Physiological aspects of racewalking include studies of energy costs (Brisswalter et al., 1998; Hagberg and Coyle, 1984; Cavagna and Franzetti, 1981) and of muscle activity or electromyography (MacLellan and Patla, 2006; Marigold and Patla, 2005; Murray et al., 1983).

A significant advance in footfall load analysis in running was the inverted pendulum model in plane motion, proposed by Blickhan (1989) and illustrated by McMahon and Cheng (1990), Farley and Gonzalez (1996), Lee and Farley (1998), and Arampatzis et al. (1999). In this model, the body mass  $m$  was lumped at the hip joint, and the leg–foot assembly was represented as an undamped linear compression spring in plane motion about a fixed pivot on a rigid surface. Gerritsen et al. (1995), and Rapoport et al. (2003) investigated more complex multiple linkage models.

The role of track compliance in reducing the initial transient heel-induced load spikes in running was recognized by McMahon

and Greene (1979). Increased leg stiffness  $\bar{k}$  with decreased track compliance  $k_s$  in steady running was observed by Kerdok et al. (2002) and Ferris et al. (1998). See Table 1. Body dynamics for one-step walking or running from a rigid to a compliant surface were measured by MacLellan and Patla (2006), Marigold and Patla (2005), and Ferris et al. (1999).

Except for the ground reactions measured by Wilson et al. (1997), who used unshod subjects, it appears that all of the studies cited above involved subjects wearing sports shoes. Since sports shoes vary greatly in design (their compression compliance is typically 200–400 kN/m) the meaning of ground reaction data of shod subjects on compliant surfaces becomes clouded. Since all subjects in the present studies were barefoot, shoe compliance did not contaminate our response data. Unlike previous studies, the new inverted pendulum model formulated herein includes nonlinear leg damping, initial spikes in leg stiffness, and a forward moving foot pivot on a compliant mat. By identifying these physical parameters through this new mathematical model, the main purpose of this study could be achieved: to determine the role of footfall surface compliance on the foot reactions, especially the initial spike loads.

### 2. Methods

#### 2.1. Dynamic simulation

For a barefoot subject racewalking or running on a horizontal, rigid surface (a steel force plate), gait can be characterized by measured footfall reaction loads defined in Fig. 1. Here the vertical load is  $f_v(t)$  and the anterior–posterior (braking–propulsive) load is  $f_a(t)$ , each normalized by the subject's body weight,

\* Corresponding author. Tel.: +1919 489 3041.

E-mail address: [jwilson@duke.edu](mailto:jwilson@duke.edu) (J.F. Wilson).

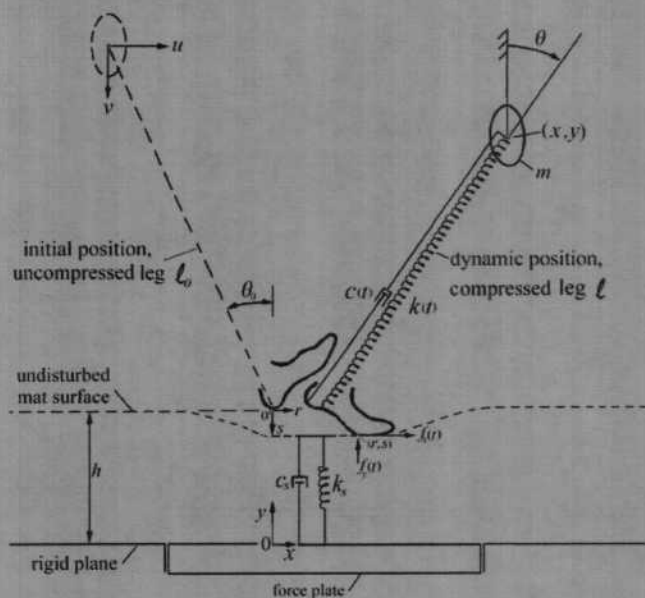


Fig. 3. The lumped mass, inverted pendulum, and mat surface model.

$$l' = [(x-r)(x'-r') + (y-h+s)(y'+s')]/l \quad (6)$$

The hypothesized form for  $r = r(t)$  and its forward velocity during  $t_c$  are  $r = r_0 t(2 - t/t_c)/t_c$ ;  $r' = 2r_0(1 - t/t_c)/t_c$  (7)

The amplitude  $r_0$  is a fraction of the foot length. The foot's forward velocity upon touch down is  $2r_0/t_c$  and is zero at lift-off.

The respective foot loads in the  $x$  and  $y$  directions, with their initial and terminal conditions, are

$$f_x(t) = c'l' \sin \theta + k(\ell_0 - \ell) \sin \theta; f_x(0) = f_x(t_c) = 0 \quad (8)$$

$$f_y(t) = c'l' \cos \theta + k(\ell_0 - \ell) \cos \theta; f_y(0) = f_y(t_c) = 0 \quad (9)$$

Further,  $\theta(0) = \theta_0$  and  $y'(0) = -v$  at touch down, where  $y'(t_c) \approx v$  at lift-off. If  $\theta_0$  is nearly the same at  $t = 0$  and at  $t = t_c$ , and changes in  $\ell_0$  are small, then the forward distance traveled by  $m$  at constant velocity  $u$  in time  $t_c$  is given by  $2\ell_0 \sin \theta_0 = ut_c$ . Thus

$$\theta_0 \approx -\sin^{-1}(0.5ut_c/\ell_0) \quad (10)$$

If the magnitudes of the initial and terminal vertical velocities are about the same, then elementary impact-momentum theory can be used to estimate  $v$ . Thus

$$v = \frac{1}{2m} \int_0^{t_c} (f_y(t) - mg) dt = \frac{t_c g}{2} \left( \frac{\int_0^{t_c} f_y(t) dt}{mg} - 1 \right) \quad (11)$$

Here,  $\overline{f_y(t)}$  is the measured mean value of the vertical reaction load.

Given  $\theta_0$ ,  $v$ ,  $c = c(t)$ ,  $k = k(t)$ ,  $\hat{P} = \hat{P}(t)$ ,  $c_s$ , and  $k_s$ , then (1–3) are solved numerically for  $(x, y, s)$ , subject to conditions (4–7). From these solutions, the foot reaction loads are computed from (8) and (9), which should match their respective measured traces  $f_x(t)$  and  $f_y(t)$ . Analytical forms for  $c$ ,  $k$ ,  $\hat{P}$ ,  $c_s$ ,  $k_s$  are now discussed.

2.1.1. Forms for damping

A two-part leg damping function is hypothesized as

$$c = c(t) = c_a[1 - \exp(-900t)] + c_b \sin(2\pi t/t_c) \quad (12)$$

Here  $c_a$  and  $c_b$  are positive constants and  $c(0) = 0$ . The coefficient of  $c_a$  is essentially constant for  $t > 0.01t_c$  s. Define  $\bar{k}$  as the mean value of  $k$ , and define

$$\zeta = \frac{c_a}{2\sqrt{km}} \quad (13)$$

A similar expression for a mat's damping factor is defined as

$$\zeta_s = \frac{c_s}{2\sqrt{k_s m}} \quad (14)$$

2.1.2. Forms for stiffness

Measurements of  $\bar{k}$  for various running scenarios are compiled in Table 1. However, if  $\bar{k}$  replaces  $k$  in Eqs. (1–9), their solutions do not produce the initial spike responses for heel strikers as observed in Figs. 1 and 2. To produce these spikes, characterize the leg-foot stiffness as

$$k(t) = \bar{k} + \hat{k}(t) \quad (15)$$

A number of spikes  $N$  can be represented as a sum of  $i$  stiffness spikes, or

$$\hat{k}(t) = \sum_{i=1}^N k_i \sin^5(0.5\pi t/t_i) \text{ if } 0 < t < 2t_i \\ = 0 \text{ otherwise} \quad (16)$$

in which  $k_i$  is the amplitude and  $t_i$  is the time required to reach this peak value. Examples of two-component stiffness spikes ( $N = 2$ ) for the racewalking and for running simulations are shown as inserts in Figs. 4 and 5.

The horizontal, spike-mitigating load is hypothesized as

$$\hat{P} = -f_0 \hat{k}(t)(\ell_0 - \ell) \sin \theta; \quad 0 < f_0 < 1 \quad (17)$$

Here the fraction  $0 < f_0 < 1$  is an empirical constant. When (15) and (17) are combined with (1), the latter equation becomes

$$m\ddot{x}' = c'l' \sin \theta + [\bar{k} + (1 - f_0)\hat{k}(t)](\ell_0 - \ell) \sin \theta; \\ x(0) = \ell_0 \sin \theta_0; \quad \dot{x}(0) = u \quad (1')$$

This result clearly shows the reduction in  $\hat{k}(t)$  for positive fractional values of  $f_0$ . Eq. (8) is likewise recast to reflect the spike mitigation for the horizontal foot reaction load, or

$$f_x(t) = c'l' \sin \theta + [\bar{k} + (1 - f_0)\hat{k}(t)](\ell_0 - \ell) \sin \theta; \\ f_x(0) = f_x(t_c) = 0 \quad (8')$$

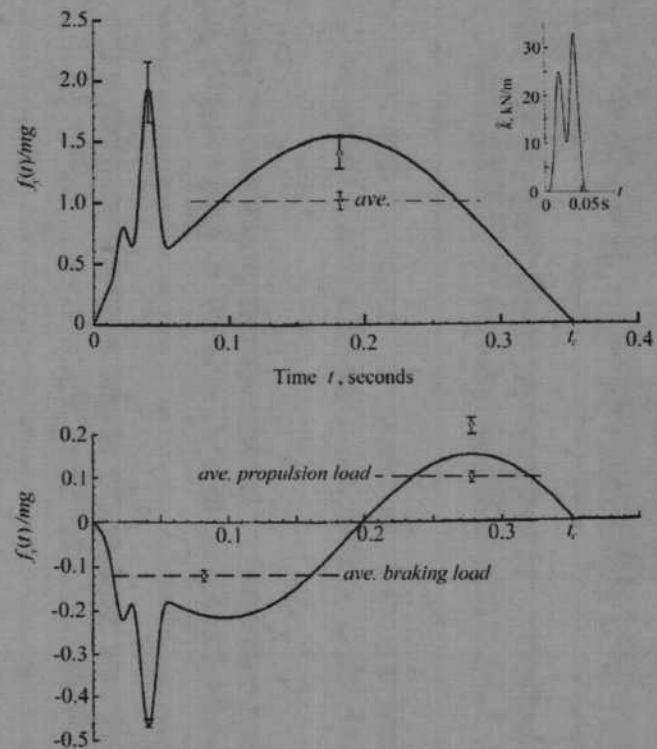


Fig. 4. Data (open circles) and simulations (continuous lines) depict footfall loads for barefoot racewalkers on a rigid force plate. Vertical bars on the open circles are  $\pm 1$  sd for the measured mean attribute over all subjects. Inset is the best-fit, transient dual spiked leg-foot stiffness needed to simulate the measured load responses.

In (2), (3) and (9),  $k = k(t)$  is simply defined by (15). For judicious choices of  $\bar{k}$ ,  $\bar{k}$  and  $f_0$ , the computed response loads  $f_x(t)$  and  $f_y(t)$  correlate with their respective measured time histories.

The mechanical properties for the four foamed polymer mats (Wilson, 2006) are summarized in Table 2. For racewalking on mats, the average vertical impact velocity  $\bar{v}$  is sufficiently small that the strain rate in compression can be approximated as  $\dot{\epsilon} = \bar{v}/h \approx 0$ , and static measures of  $(c_s, k_s)$  are used. For running on mats,  $\bar{v} \approx 0.2$  m/s, which leads to  $\dot{\epsilon} \approx 35$  s<sup>-1</sup>, and the dynamic measures of  $(c_s, k_s)$  are used. Further,  $\xi_s = 0.258$  for all four mats (Wilson, 2006). The other system parameters are listed in Table 3.

2.2. Experiments

Three healthy volunteer male athletes, two nationally ranked in racewalking and running, participated in the experimental trials. For these subjects, the mean values for age, body mass, and leg length were: 31.3 yr, 68.8 kg, and 0.997 m. For each of the two gaits and for each of the four mats of Table 2 covering the force plate, there were nine like trials: three trials for each of the three subjects. The subjects were all heel strikers and always barefoot. They effected all trials at a forward speed of  $2.5 \pm 0.1$  m/s, measured with a stopwatch as the subject traversed

the 10 m runway leading to a 900 Hz Kistler force plate. A video camera recorded each force plate footfall, to give evidence that slip did not occur for either the impacting foot or the foamed polymer mat. Each of the respective eight attributes was averaged arithmetically and the standard deviation (sd) was computed across the nine like trials. The computer system used for storing and evaluating the force plate data such as shown in Fig. 1 is described in detail by Rochelle (1992).

3. Results

3.1. Racewalking: rigid surface

The mean attribute data based on three trial runs for each of the three barefoot racewalkers on the rigid steel surface of the force plate are shown as in Fig. 4 as open circles. The ordinates were normalized by the subjects' mean body weight:  $mg = 675$  N. The vertical load spike of 1.905 has the largest standard deviation ( $sd = 0.254$ ) of all attributes; and  $t_c = 0.3503$  s ( $sd = 0.0308$ ).

The solid curves of Fig. 4 were computed from (8') and (9), based on numerical solutions to (1') and (2) and the constraints (4–7). For each solution there were four fixed measured parameters:  $(m, \ell_0, t_c, u)$ . The 11 best-fit parameters (the numbers are listed in the left column of Table 3) were computed using Mathematica (Wolfram, 1999), employing a direct search method designed to avoid local maxima/minima.

This dynamic simulation for racewalking shows agreement to the measurements to within  $\pm 1$  sd for all but one attribute: the peak propulsion load, which is underestimated. Here, the leg stiffness  $\bar{k}$  was computed as 10.8 kN/m, which is within the range of 7–16.3 kN/m for runners, as measured by Farley and Gonzalez (1996) (Table 1). Our new data include the racewalker's initial transient leg-foot stiffness spikes: 25 and 35 kN/m each, lasting for 0.04 s; and the leg damping parameters:  $c_a = 10$  N s/m and  $c_b = 17.5$  N s/m. From (13) the mean leg damping factor is  $\xi = 0.00583$  or about 0.6%. Also, because of its sinusoidal component, the overall damping increased in the first half of the impact cycle, and then became negative for a short time in the second half of the impact cycle, which models the reversal of the curvature for  $f_y(t)$  as  $t \rightarrow t_c$ . Other characteristics of the racewalker are: (1) the initial vertical velocity of the impacting foot is small ( $v = -0.06$  m/s) and the terminal velocity at lift-off is also small; (2) the pivot of the impacting foot moves forward 12 cm, heel to toe; (3) the forward-moving pivot reduces the initial anterior spike stiffness by a factor of (1–0.7), or by 30%.

3.2. Running: rigid surface

The data analogous to that of Fig. 4, but for the barefoot runners on the rigid force plate, are shown in Fig. 5. Here,  $t_c = 0.2892$  s ( $sd = 0.0191$ ) was smaller than for racewalking, where the time deficit was applied to the flight phase in running to maintain the same forward speed of 2.5 m/s. The solid curve simulations were computed in the same way as for racewalking. The 11 best-fit running parameters (rigid surface) are listed in

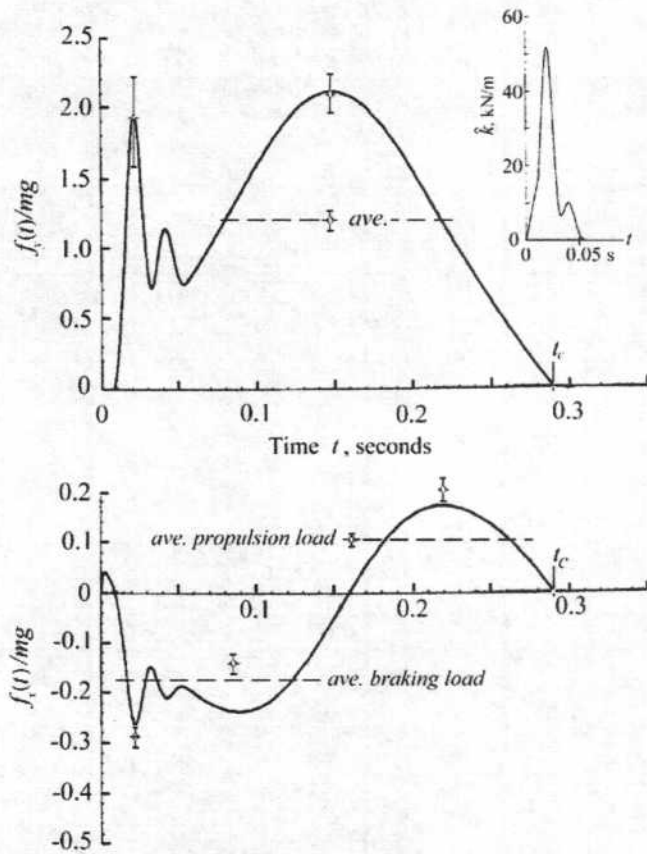


Fig. 5. Data (open circles) and simulations (continuous lines) depict footfall loads for barefoot runners on a rigid force plate. Vertical bars on the open circles are  $\pm 1$  sd for the measured mean attribute over all subjects. Inset is the best-fit, transient dual spiked leg-foot stiffness needed to simulate the measured load responses.

Table 2 Properties of the foamed polymer mats.  $\xi_s = 0.258$  in all cases (Wilson, 2006).

Mat type	Density (kg/m <sup>3</sup> )	Thickness (mm)	Static properties $\dot{\epsilon} \approx 0$		Dynamic Properties $\dot{\epsilon} \approx 35$ s <sup>-1</sup>	
			$c_s$ (kN s/m)	$k_s$ (kN/m)	$c_s$ (kN s/m)	$k_s$ (kN/m)
Black	481	4.86	4.30	1010	4.95	1340
Blue	451	6.40	3.73	758	4.31	1020
Red	421	5.30	3.89	824	4.34	1030
White	370	7.00	2.21	266	2.47	334

**Table 3**Best-fit system parameters (first 11 rows) for four simulations. For each simulation,  $m = 68.8$  kg,  $l_0 = 0.997$  m, and  $u = 2.5$  m/s were fixed.

Parameter	Symbol (units)	Racewalking rigid	Surface white mat	Running rigid	Surface blue mat
Leg damping:					
	$c_d$ (N s/m)	10.0	10.0	100	100
	$c_b$ (N s/m)	17.5	17.5	175	175
Leg stiffness:					
	$\bar{k}$ (kN/m)	10.8	10.7	12.9	11.3
	$s_1$ (kN/m)	25.0	17.5	52.0	33.8
	$s_2$ (kN/m)	33.0	23.1	10.0	6.5
	$t_1$ (s)	0.02	0.02	0.02	0.02
	$t_2$ (s)	0.04	0.04	0.04	0.04
Foot pivot:					
	$f_0$	0.70	0.42	0.66	0.65
	$r_0$ (cm)	12.0	12.0	2.0	1.0
Initial values:					
	$v$ (m/s)	-0.060	-0.060	-0.295	-0.295
	$\theta_0$ (rad)	-0.371	-0.371	-0.371	-0.371
Stance time: (measured)					
	$t_c$ (s)	0.350	0.355	0.289	0.306
Peak vertical displ. of $m$ : (computed)					
	$y_p$ (m)	0.9429	0.9481	0.9596	0.9491

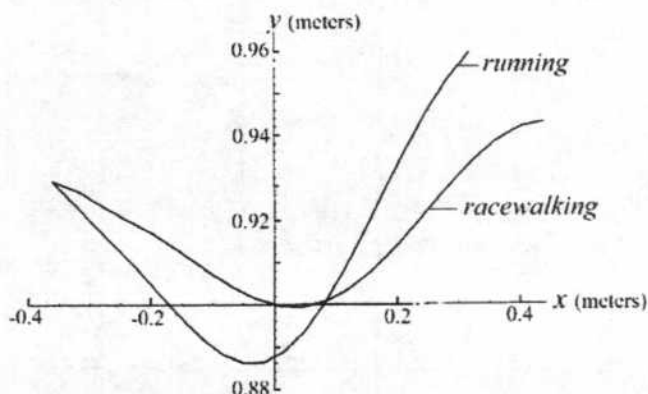
**Fig. 6.** Computed hip joint trajectories for barefoot racewalkers and runners on a rigid force plate, where  $u = 2.5$  m/s.

Table 3. The most significant differences in responses between the two gaits are seen by comparing Figs. 4 and 5: running produces higher values for the active vertical peak, for the average vertical load, and for the average braking load. However, running requires a lower peak braking load. The higher values for three of the four load attributes reflect the higher average leg stiffness for running:  $\bar{k} = 12.9$  kN/m, compared to  $\bar{k} = 10.8$  kN/m for racewalking. Other differences include the average leg damping factors  $\zeta$ : 5.67% for running and 0.583% for racewalking; and the foot-pivot movement  $r_0$ : 2.0 cm for the running compared to 12 cm for racewalking. This last result indicates that the racewalkers had a more exaggerated heel-toe motion than the runners, who in the present trials landed almost flat-footed.

Shown in Fig. 6 are the calculated body mass trajectories for the barefoot racewalkers and the runners on the rigid surface of the force plate. For these gaits, the starting point and other initial conditions were the same, although the stance times were different. During stance, the racewalker's forward displacement  $x$  was larger; however, the runner had elevated his body mass further in the  $y$ -direction. This latter observation is consistent with an initial runner's velocity (downward, just prior to heel contact) of 0.295 m/s, which is significantly higher than the counterpart velocity of 0.06 m/s for the racewalker, who runs

closer to the ground plane, and whose heel drops less far before surface contact.

### 3.3. Mat surface: measured effects

For each of the two gaits and for each of the four mats of Table 2 covering the force plate, there were nine like trials: three trials for each of three subjects. Each of the respective eight attributes was averaged arithmetically across the nine like trials. Consider the most significant results.

- (1) Regardless of the type of mat, the five attributes showed at most a  $\pm 1\%$  variation from the respective attribute for the rigid surface cases. Those nearly constant attributes were  $t_c$ , the peak active vertical load, and the three average loads: vertical, braking, and propulsion.
- (2) The main effects of the mats were to reduce the vertical spike, the braking spike, and the active peak propulsion load, as shown in Fig. 7 for racewalking and in Fig. 8 for running.
- (3) Consider the mat properties listed in Table 2. The white mat, the one with the lowest density ( $370$  kg/m<sup>3</sup>) and least compression stiffness ( $k_s = 266$  kN/m), was the most effective mat for reducing the vertical and braking spike loads for racewalking, with respective reductions of about 12% and 14%. However, for running on the same white mat the reductions were less dramatic, with spike reductions of 7.5% and 9%.
- (4) The blue mat, which had intermediate values for both density ( $450$  kg/m<sup>3</sup>) and compression stiffness ( $k_s = 1020$  kN/m), was the most effective mat for reducing the vertical and braking spike loads for running. For these attributes, the respective reductions were about 12.5% and 17%.

### 3.4. Mat surface: simulations

Dynamic simulations were carried out for the two mats that showed the most dramatic reductions in the peak response loads: the white mat for racewalkers and the blue mat for runners. The computation scheme to identify the 11 best-fit system parameters to the attribute data was the same as previously described, except that Eq. (3), which incorporated the mat properties ( $k_s, c_s$ ), was now included.

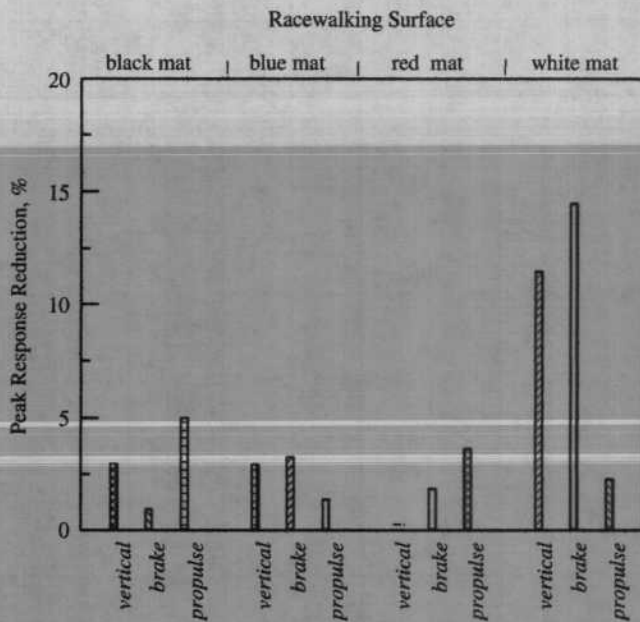


Fig. 7. Measured reductions in peak foot load responses for racewalkers on four different foamed polymer mats, as compared to their counterpart measures for racewalkers on a rigid surface.

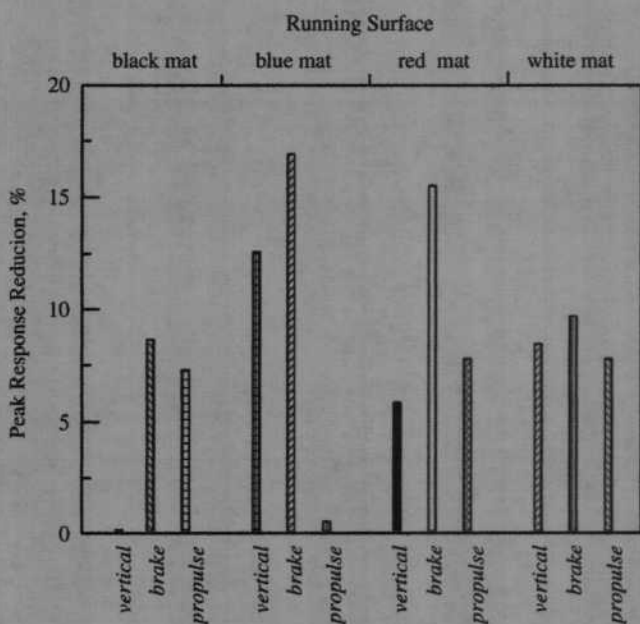


Fig. 8. Measured reductions in peak foot load responses for runners on four different foamed polymer mats, as compared to their counterpart measures for runners on a rigid surface.

Listed in Table 3 are the 11 best-fit parameters for white and blue mats for the two gaits, the stance times  $t_c$ , the computed peak vertical displacement  $y_p$  for  $m$ , and the three measured parameters common for all calculations:  $(m, t_0, u)$ . The results of these calculations are summarized.

(1) For racewalkers on the white mat, the leg stiffness was modified:  $\bar{k}$  was reduced only a little, from 10.8 to 10.7 kN/m;

but both  $s_1$  and  $s_2$  were reduced by a factor of 0.7. Also, the horizontal leg stiffness spike-mitigating factor  $f_0$ , as defined by Eq. (17), was reduced from 0.7 to 0.42.

(2) For runners on the blue mat, the leg stiffness was modified:  $\bar{k}$  was reduced from 12.9 to 11.3 kN/m; and both  $s_1$  and  $s_2$  were reduced by a factor of 0.65. Further,  $f_0$  was reduced from 0.66 to 0.65; and the foot forward roll amplitude  $r_0$  was reduced from two to one centimeter.

#### 4. Discussion

We found that the computed trajectories for the lumped mass  $m$  for the racewalking and running subjects on our compliant surfaces were nearly the same as those trajectories in Fig. 6 for these same subjects traversing a rigid surface. In particular,  $y_p$ , or the peak vertical displacement of  $m$ , increased by only 0.55% when racewalking on the white mat instead of the rigid force plate; and  $y_p$  decreased by about 1.1% when running on the blue mat instead of the rigid surface. The computed displacements are listed as  $y_p$  in Table 3. These results are consistent with the measurements of Ferris et al. (1998), who observed that the height of the center of body mass for runners remained nearly constant for different running surfaces. They also observed that leg stiffness  $\bar{k}$  was higher on their much softer surfaces, for  $k_s$  in the range 15–62 kN/m (see Table 1). Had Ferris et al. included the subjects' shoe compliance, their reported range of  $k_s$  would have been even lower. We found a negligible dependency of leg stiffness on surface compliance probably because our  $k_s$  values were about an order of magnitude higher (see Table 2), and our subjects were unshod.

In reviewing the related open literature, we noted that researchers rarely if ever reported the compressive dynamic-dependent properties for either their surface mats (some used dynamic-independent spring-loaded track surfaces), or for their subjects' sports shoes. In our data analysis, we employed the dynamic properties of the foamed polymer mats (see Table 2). We also note that the effective  $k_s$  would decrease if the subjects were shod, since the shoe and mat compliances are in series. Our present studies have eliminated these two sources of data contamination.

Regardless of gait and surface, the heel striking subjects always produced initial transient reaction spikes. Consider the insert of Fig. 2, the skeleton of a heel striker's foot. Glasoe et al. (1999) suggest that such spikes from heel strikers are dissipated as the first ray is lowered to the ground in early stance. The first ray is a single foot segment consisting of the first metatarsal and the first cuneiform bones. Further studies needed to clarify this physical phenomenon.

Our studies showed that foamed polymer mats reduced both transient vertical heel load spikes and the horizontal foot reactions during braking and propulsion. Further, barefoot racewalkers and barefoot runners required mats of different compliance to achieve the optimal or best reductions in load. Still to be determined are the best footwear-surface compliance combinations which minimize spike-induced injuries and also follow the design guidelines for modern compliant tracks producing the best running times.

#### Conflict of interest statement

Concerning the manuscript, footfall force data for barefoot fitness walkers on compliant surfaces, there is not now and there never was any conflict of interest regarding this research.